

THREE DIMENSIONAL GOLF BALL FLIGHT

Anastas Ivanov¹, Juliana Javorova²

¹*Todor Kableshkov University of Transport, Sofia, BULGARIA, aii2010@abv.bg*

²*University of Chemical Technology and Metallurgy, Sofia, BULGARIA, july@uctm.edu*

Abstract: *The three dimensional (3D) flight of a golf ball at taking into account the Magnus effect is studied in the paper. For this purpose it is composed a system of six nonlinear differential equations. To determine the 3D orientation of the ball the rotations around all three axes are given by the so-called Cardan angles instead of classical Euler ones. The high nonlinear system differential equations are solved numerically by a special program created in the MatLab-Simulink environment. It is founded the laws of motion, velocities and accelerations on all six coordinates, as well as the projections of trajectory on the three coordinate planes. The presented analytical base and numerical results in the paper increasing and expanding the knowledge in the theory of general motion of spherical solid and leads to new more extensive research in this complicated area.*

Keywords: *three dimensional flight, golf ball, drag and lift forces, Magnus effect, MatLab*

1. Introduction

In a current time a lot of publications about studies of a golf ball flight in air environment are known. A large part of the papers can be generalized as research on the aerodynamics (as a whole) of the ball flight but the other studies can be assigned to some specific fields. The first of them is related to the biomechanics of the stroke with a club from the side of the golfer [1, 2, 3, etc.]. The publications from the second field deal with the impact between the club head and the ball and the influence of this interaction on the ball flight after that [4, 5, etc.]. The other group of authors put the accent on the investigation of the mechanical properties and damping characteristics of the balls materials [6, 7, 8, etc.]. Furthermore in some of the studies [9, 10, 11, etc.] the focus is on the location, density, size and shape of the ball dimples, as well as their influence on the drag and lift coefficients in dependence of the ball velocity and Reynolds number.

By the other hand, a feature of most studies is that the flight of the golf ball in the air environment is considered as a material point motion [12, 13, 14, 15, etc.]. A reason for this

gives them the fact that the golf ball is a relatively small in size. In the above mentioned papers the golf ball flight is described by three differential equations about the three axes of the Cartesian coordinate system. Furthermore some of the solutions [9, 10] refer to golf ball motion only in one plane (the vertical one). Such approaches are not so precise, since the real motion of the ball is three dimensional and because of which it is necessary to consider a dynamic model with six degrees of freedom. One solution for such 3D model is presented in [16] at studying the tennis ball flight. Here it is important to mention that with similar mathematical models which are linearized with respect to the angular rotations are studied the 3D vibrations of the individual movable parts of the machine structures, or even entire aggregates connected by elastic elements [17 and many others].

In relation with the above mentioned the aim of the current work is to study the 3D golf ball flight in air environment, as the moving ball is considered as motion of the material body in air environment with aerodynamic resistances. For this purpose the characteristics of the golf ball are identified, the mathematical

model with six degree of freedom is composed, the numerical solution and results are presented and discussed.

The flight is studied without taking into account a number of additional factors affecting the golf stroke as: type and size of the golf-club, a ball design, individual sporting and professional skills of the golfer, etc. The parameters of the presented solutions are selected according to actual features of the golf game.

2. Golf ball characteristics

In order to start a study of the golf ball flight it is necessary to know the geometrical and mechanical characteristics of the ball. The racing golf ball has a mass no more than $45,93 \cdot 10^{-3}$ [kg] and has a diameter not less than $4,267 \cdot 10^{-2}$ [m]. The golf ball must also have the basic properties of a spherically symmetrical body [18]. It means that the ball itself must be spherical and must have a symmetrical arrangement of dimples on its surface. There are official documents with additional restrictions, such as radius and depth of dimples, maximum launch speed from test apparatus and maximum total distance when launched from the test equipment. Most golf balls today have about 250÷450 dimples, though there have been balls with more than 1000 dimples (Fig.1). Usually the golf balls are designed to be as symmetrical as possible. But asymmetrical design helped the ball to change its trajectory during the flight.

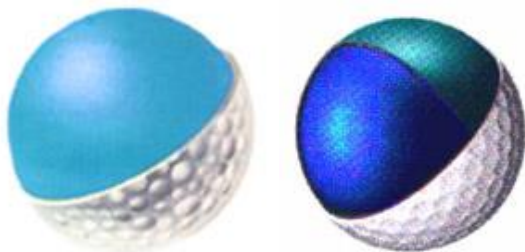


Figure 1: *Some golf ball constructions*

The presence of the dimples on the golf ball surface makes a larger air cover which moves

simultaneously with a ball. By this way, at interaction of the golf ball and air during the flight the contact area “fluid-fluid” rises and the friction reduces. This leads to a significant reduction of the aerodynamic resistance (or so called drag) and respectively to increasing of the length, height and time of the golf ball flight. In the last years different kind of dimpled golf balls appeared as they differs mainly by the size, shape and density of the dimples. Here must be emphasizing that according to [10] these dimpled balls induce higher values of the drag coefficient C_D but also a bigger lift-to drag ratio.

The golf balls can be differently designed (Fig.1). The most used ones are two layers balls: a large inner core of a dense material (rubber or similar) and a thin hard cover (cut-proof Surlyn) as a second outer layer. These balls combine durability with maximum distance as well as lower spinning. Lately the golf balls construction is multilayered (three, four layers). Three layered balls typically have Surlyn or a softer polyurethane cover and a mantle layer of rubber windings around a rubber core. Four layered balls additionally have an inner cover made of a blend of ionomers and an outer cover made of Elastomer or Balata. Having more layers helps to easily implement the ball spin and Magnus effect. Or shortly, with multilayer balls it is possible to achieve a smaller distance of the flight but the golfer has a greater opportunity to change the flight trajectory.

As additional information here must be note that in the golf game are used nine different kinds of the golf strokes (push, push slice, push hook; slice, straight, hook; pull, pull slice, pull hook) which lead to different kind of the ball flights trajectory.

In the current paper will be considered the classical case of two layered golf body, as for the study the following assumptions are introduced: the golf ball is a solid sphere with an average radius $R = 2,14 \cdot 10^{-2}$ [m], mass $m = 4,59 \cdot 10^{-2}$ [kg] and corresponding to these values mass moment of inertia J [kg.m²].

By the kinematic and dynamic point of view, based on the above assumptions, the flight of the golf ball can be considered as a general motion of a solid sphere (which is accepted as a perfectly rigid body) in unalterable air environment without wind. The air resistance is taken into account by external to the golf ball forces and moments.

3. Mathematical model

3.1. Elements of the golf ball Kinematics

The golf ball has six degrees of freedom. Its laws of motion about fixed coordinate system $Oxyz$ are presented by six functions of the time, (Fig. 2):

$$x = x(t), y = y(t), z = z(t) \quad (1)$$

$$\psi = \psi(t), \theta = \theta(t), \varphi = \varphi(t) \quad (2)$$

From the laws of motion (1), which define the position of the mass ball center, after excluding the time t , its trajectory is obtained. Further in the text, this trajectory of the gravity center of the ball is called shortly trajectory.

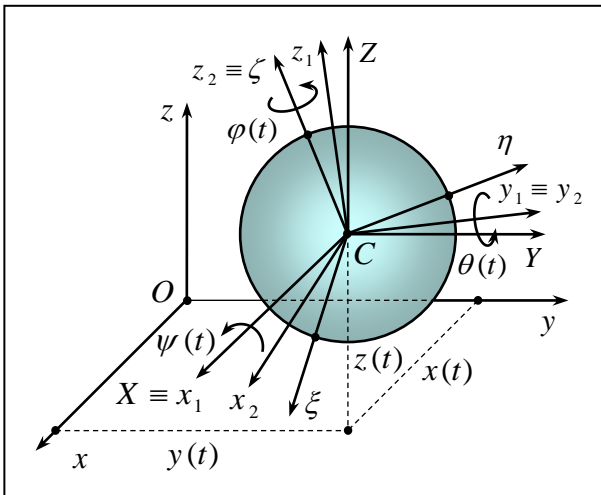


Figure 2: Golf ball laws of motion

It is accepted that the three angular functions can be assigned with Cardan angles in their traditional form: rotation of angle $\psi(t)$ about axis X , rotation of angle $\theta(t)$ about axis $y_1 \equiv y_2$ and finally rotation of angle $\varphi(t)$ about axis $\zeta \equiv z_2$.

The ball angle velocity $\omega(t)$ is defined by its algebraic projections on axes of the translation movable coordinate system $CXYZ$, which are usually called kinematic equations:

$$\omega_x = \dot{\psi} + \dot{\varphi} \cdot \sin \theta, \quad (3.a)$$

$$\omega_y = \dot{\theta} \cdot \cos \psi - \dot{\varphi} \cdot \cos \theta \cdot \sin \psi, \quad (3.b)$$

$$\omega_z = \dot{\varphi} \cdot \cos \theta \cdot \cos \psi + \dot{\theta} \cdot \sin \psi. \quad (3.c)$$

3.2. Elements of the golf ball Dynamics

During the golf ball flight in the air environment, the following forces act on the movable object, (Fig. 3).

Weight force G :

$$\mathbf{G} = m \cdot \mathbf{g} \quad (4)$$

Aerodynamic resistance (drag) force F_D :

This force act in the direction opposite to the velocity \mathbf{v} and it is determined by the square of this velocity, namely:

$$\mathbf{F}_D = -\frac{1}{2} \cdot C_D \cdot \rho_a \cdot A \cdot \mathbf{v} \cdot \mathbf{v} = -k_D \cdot \mathbf{v} \cdot \mathbf{v}, \quad (5)$$

$$F_D = \frac{1}{2} \cdot C_D \cdot \rho_a \cdot A \cdot v^2 = k_D \cdot v^2. \quad (6)$$

Here \mathbf{v} is the velocity of the center of gravity of the ball, C_D - dimensionless drag coefficient, ρ_a - air density, A - area of the middle cross-section of the ball. On the other hand, the introduced coefficient k_D is a function of the drag coefficient, air density and the area.

The air density ρ_a depends on the environment temperature and it is accepted by the average value $\rho_a = 1,205 \text{ [kg/m}^3]$ at $t = 20 \text{ [}^\circ\text{C]}$. The middle cross-section area A of the ball for the considered case is $A = \pi \cdot R^2 = 16,619 \cdot 10^{-4} \text{ [m}^2]$.

The aerodynamic resistance coefficient C_D , or so called drag coefficient, depends on the Reynolds number Re . It is well known that Re characterizes the turbulent conditions and

on the other hand it is a function of the ball linear velocity. Here must be noted that a detailed study of the drag coefficient C_D for dimpled and grooved golf balls is presented in the paper [10], where this coefficient is studied in dependence of the ball motion characteristics (velocity v , Reynolds number Re and revolutions per minute n). Under the

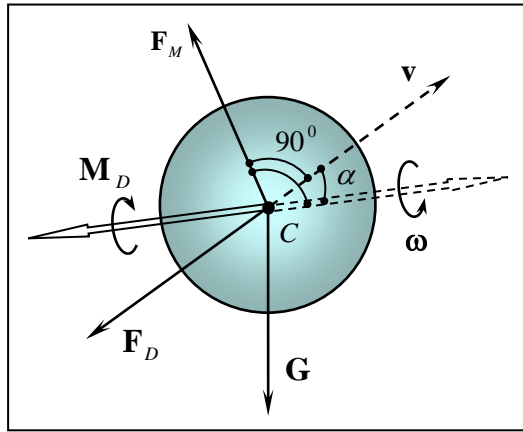


Figure 3: Forces acting of the golf ball

chosen here circumflow conditions $n = 0 \div 400$ [rpm], $v = 20 \div 60$ [m/s], $Re = (2 \div 5) \cdot 10^5$, the coefficient C_D has relatively constant values and it is possible to accept the averaged value of it, namely $C_D = 0,30$.

Magnus (lift) force F_M :

This force takes into account the pressure difference that is created by the air stream flowing around the ball, in the two opposite areas normally arranged about the plane formed by the vectors of linear velocity \mathbf{v} and angular velocity $\boldsymbol{\omega}$. The Magnus force (or so called lift force) is determined by:

$$\mathbf{F}_M = \frac{1}{2} \cdot C_L \cdot \rho_a \cdot A \cdot \frac{\boldsymbol{\omega} \times \mathbf{v}}{|\boldsymbol{\omega} \times \mathbf{v}|}, \quad (7)$$

$$k_L = \frac{1}{2} \cdot C_L \cdot \rho_a \cdot A \cdot \frac{1}{|\boldsymbol{\omega} \times \mathbf{v}|}. \quad (8)$$

where C_L is the lift coefficient, ρ_a is the air density and A is the middle cross-section area. (Fig. 3). As a first approach of the current

problem solution, the lift coefficient C_L can be assumed as value approximately twice less in comparison with the drag coefficient. The coefficient k_L depends on C_L , ρ_a , A and the magnitude of the vector $\boldsymbol{\omega} \times \mathbf{v}$.

It is essential to note that the effect of the Magnus force (often called Magnus effect) can be positive or negative in dependence of the directions of the linear velocity vector \mathbf{v} and angular velocity vector $\boldsymbol{\omega}$. Furthermore it is possible also the case without Magnus effect when the angular velocity is zero. The above mentioned three cases related to the Magnus effect are presented schematically on Fig. 4.

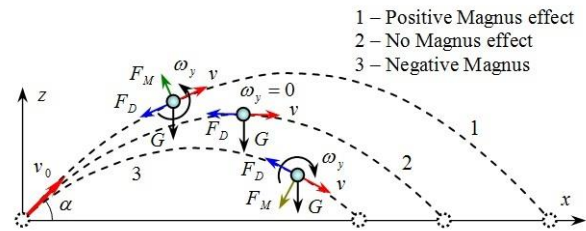


Figure 4: Magnus effect cases

Aerodynamic resistance moment M_D :

This moment (called also drag moment) acts in an opposite direction of the angular velocity $\boldsymbol{\omega}$ and it is defined as:

$$\mathbf{M}_D = -\frac{1}{2} \cdot C_D^{(m)} \cdot \rho_a \cdot A \cdot \frac{\boldsymbol{\omega}}{|\boldsymbol{\omega}|}, \quad (9)$$

$$k_D^{(m)} = \frac{1}{2} \cdot C_D^{(m)} \cdot \rho_a \cdot A \cdot \frac{1}{|\boldsymbol{\omega}|}, \quad (10)$$

where $C_D^{(m)}$ is the so called drag moment coefficient and in the current paper it is accepted that $C_D^{(m)} \approx (1/3) \cdot C_D$. Moreover the introduced coefficient $k_D^{(m)}$ depends on $C_D^{(m)}$, ρ_a , A and the magnitude of the vector $\boldsymbol{\omega}$.

3.3. Differential equations

The systems of differential equations that describe the 3D golf ball motion, considering the ball as a solid body with six degrees of freedom, has a form:

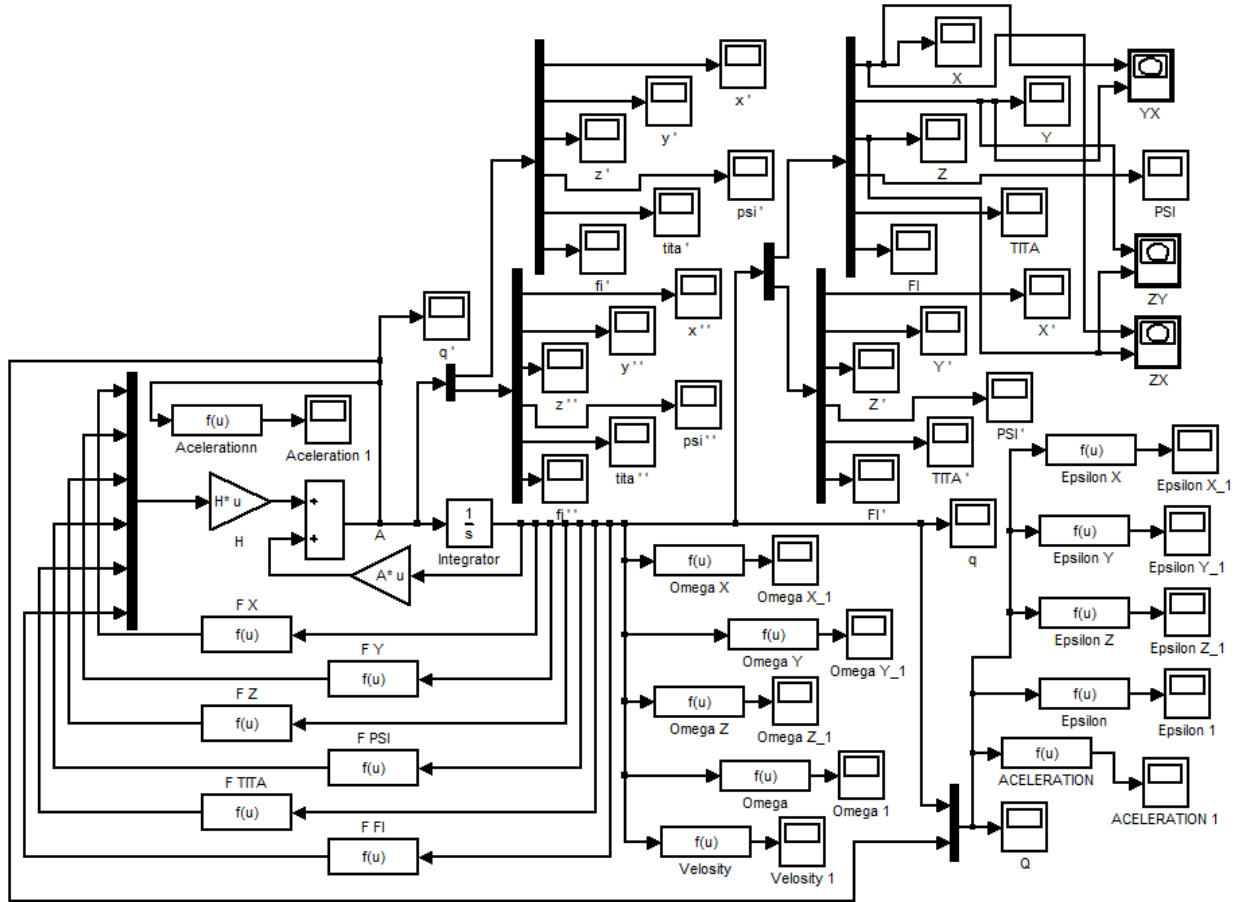


Figure 5: Simulink Block Scheme for solving the systems of differential equations (11) and (12)

$$m \cdot \ddot{x} = -k_D \cdot \dot{x} \cdot \sqrt{\dot{x}^2 + \dot{y}^2 + \dot{z}^2} + k_L \cdot (\omega_Y \cdot \dot{z} - \omega_Z \cdot \dot{y}); \quad (11)$$

$$m \cdot \ddot{y} = -k_D \cdot \dot{y} \cdot \sqrt{\dot{x}^2 + \dot{y}^2 + \dot{z}^2} + k_L \cdot (\omega_Z \cdot \dot{x} - \omega_X \cdot \dot{z});$$

$$m \cdot \ddot{z} = -k_D \cdot \dot{z} \cdot \sqrt{\dot{x}^2 + \dot{y}^2 + \dot{z}^2} + k_L \cdot (\omega_X \cdot \dot{y} - \omega_Y \cdot \dot{x}) - m \cdot g ,$$

$$J \cdot \dot{\omega}_X = -k_D^{(m)} \cdot \omega_X ; \quad (12)$$

$$J \cdot \dot{\omega}_Y = -k_D^{(m)} \cdot \omega_Y ;$$

$$J \cdot \dot{\omega}_Z = -k_D^{(m)} \cdot \omega_Z .$$

Both systems of differential equations (11) and (12) are strong nonlinear and they are connected to each other. On the other hand

their solution must be carrying out together with the kinematic equations (3).

4. Numerical solution

For the numerical integration of the systems of differential equations (11) and (12) is created a program in the MatLab–Simulink environment. The block scheme of the program is shown on Fig. 5.

As initial parameters the program regularly uses the initial conditions of the golf ball (initial position and initial angle; the latter sometimes is called in the specialized literature an elevation angle). Moreover the program works also at preliminary defined kinematic characteristics as initial linear velocity and initial angular velocity.

The program allows obtaining the following kinematic characteristics of the golf ball motion: the lows of motion about the six

coordinates $x(t)$, $y(t)$, $z(t)$, $\psi(t)$, $\theta(t)$, $\varphi(t)$, the velocity lows $\dot{x}(t)$, $\dot{y}(t)$, $\dot{z}(t)$, $\dot{\psi}(t)$, $\dot{\theta}(t)$, $\dot{\varphi}(t)$, $v(t)$, the acceleration lows $\ddot{x}(t)$, $\ddot{y}(t)$, $\ddot{z}(t)$, $\ddot{\psi}(t)$, $\ddot{\theta}(t)$, $\ddot{\varphi}(t)$, $a(t)$, the angle velocity lows $\omega_x(t)$, $\omega_y(t)$, $\omega_z(t)$, $\omega(t)$, the angle acceleration lows $\varepsilon_x(t)$, $\varepsilon_y(t)$, $\varepsilon_z(t)$, $\varepsilon(t)$, as well as the three projections of the trajectory on the coordinate planes Oxz , Oyz and Oxy , namely $z(x)$, $z(y)$ и $y(x)$.

5. Results and discussions

In the paper are presented some groups of results about the trajectory of the golf ball during the flight. First of the results refer to different values of the initial linear velocity v_0 : 20 [m/s], 40 [m/s], 60 [m/s] at keeping the constant values of the angular velocity 20,94 [rad/s] and initial angle 13 [°]. On Fig. 6 and 7 are shown the trajectories of the golf ball in the coordinate planes Oxz and Oyz , respectively. As it would be expected the largest (in height and in length) trajectory refers to the case of maximal linear velocity. The reducing of the velocity v_0 leads to decreasing of the trajectory. These tendencies are equal for both of the considered planes of motion (Fig. 6 and Fig. 7), as the height is equal of course but the length of the trajectory on x axis is definitely large compared to this on y axis.

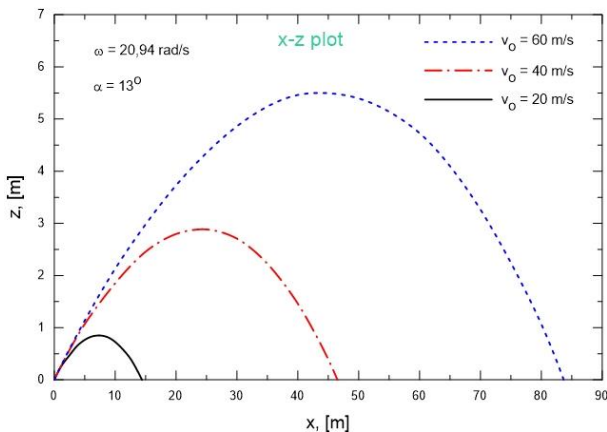


Figure 6: Trajectory of the golf ball in Oxz plane at different initial linear velocities v_0

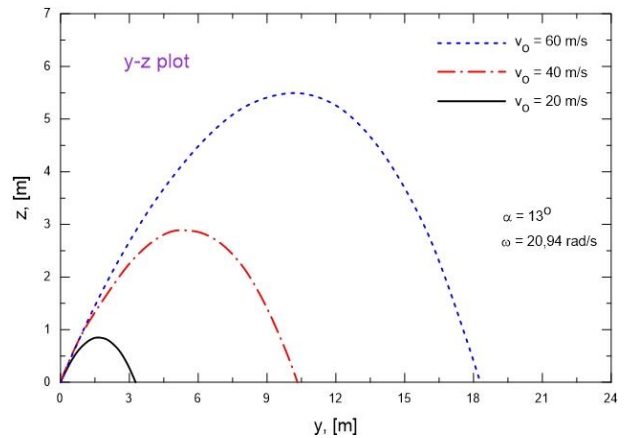


Figure 7: Trajectory of the golf ball in Oyz plane at different initial linear velocities v_0

The second groups of results are given on Fig. 8 and Fig. 9 and they demonstrate the effect of angular velocity on the model of the ball trajectory at constant initial linear velocity 50 [m/s] and constant initial angle 13 [°]. It will be considered four angular velocities ω : 0 [rad/s]; 10,472 [rad/s]; 20,944 [rad/s] and 31,416 [rad/s]. These four values of ω corresponds to the following values of n : 0 [rpm], 100 [rpm], 200 [rpm], 300 [rpm]. On Fig. 8 are presented four trajectories in the coordinate plane Oxz at values of ω_y : 0 [rad/s], 9 [rad/s], 18 [rad/s] and 27 [rad/s]. Here ω_y represent the algebraic projections of the above mentioned four different angular velocities. On the other hand on Fig. 9 the same trajectories are shown but in the plane Oyz at the same angular velocities ω . But here the algebraic projections ω_x of the considered four angular velocities are respectively, as follows: 0 [rad/s], -4,5 [rad/s], -9 [rad/s] and -13,5 [rad/s]. The negative signs here are related to the orientation of the angular velocity vector about the coordinate axis x .

The results related to the Magnus effect on the ball trajectory are presented on Fig. 10. In the case of no-spin golf stroke (black solid line) we have not the effect of Magnus force. At under-spin stroke (red dotted line; top line) the lift force acts upwards and increases the maximum height significantly. The opposite

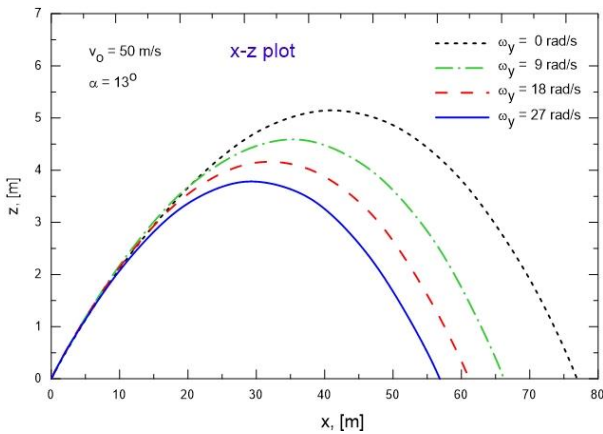


Figure 8: Trajectory of the golf ball in Oxz plane at different initial angular velocities

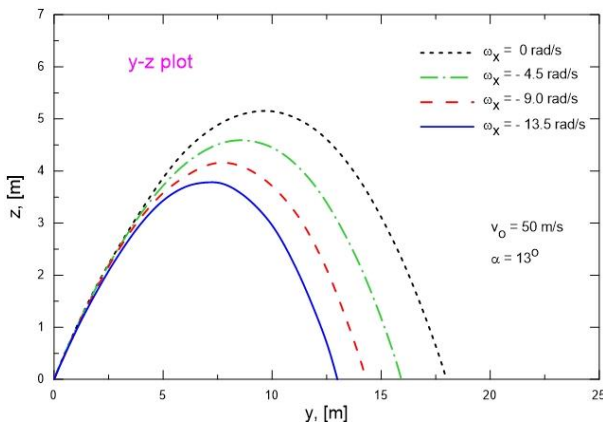


Figure 9: Trajectory of the golf ball in Oyz plane at different initial angular velocities

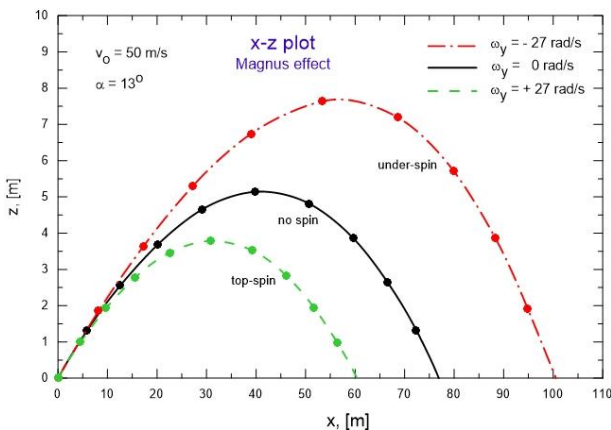


Figure 10: Magnus effect on the ball trajectory

case is a top-spin stroke (green dotted line; the lowermost line) which results in a downward Magnus force and respectively to visible decreasing of the maximum height.

As a general remark to all of the given results can be noted that the above mentioned

tendencies about the effects of different kind of velocities on the ball trajectories are in agreement with the results published in [19, 14, 10]. It is observed that here some of the trajectories profiles looks more symmetric which is based on the relatively lower values of the top-spin angular velocities.

6. Conclusion

In the paper is presented a study of 3D golf ball flight as a particular attention is paid to the Magnus effect. To conduct the research, the system of six nonlinear differential equations is composed, as it is important to mention that the golf ball is considered as a material body, not as a material point. The numerical solution is carried out by a new developed program in the MatLab-Simulink environment. The program allows to receive all possible kinematic characteristics of the golf ball flight, i.e. all lows of motion, all trajectories, all linear and angular velocities, as well as all linear and angular accelerations. Moreover by the program it is possible to receive also the generalized coordinates of the three Cardan angles and their first and second derivatives, respectively.

The effects of the initial linear velocity as well as of the initial angular velocity are investigated. From the results can be concluded that: the increasing of the initial linear velocity reflects to rising of the height and length of the ball trajectory; the increasing of the initial angular velocity (but specially for the case of top-spin rotation) leads to decreasing of the height and length of the ball flight. The analysis of the results about Magnus force effect can be generalized as follows: at under-spin rotation the trajectory visible increasing (in height and in length) compared to the no-spin rotation; it is the case of positive Magnus effect. Opposite results are received at the top-spin stroke where the trajectory visible reduces (negative Magnus effect). The significance of the presented study is expressed in the composing and using of the more complicated but more realistic model of the golf ball flight. The presented differential

equations and results are linked to the 3D motion of the solid body in air environment, not 3D motion of the projectile (material point) as the latter is not so accurate from a physical standpoint.

References

- [1] MacKenzie S.J., Springings E.J., *A three-dimensional forward dynamics model of the golf swing*, Sport Engineering, 2009, 165-175.
- [2] Zheng N., Barrentine S. W., Fleisig G. S., Andrews J. R., *Kinematic analysis of swing in pro and amateur golfers*, Int. J. Sports Med., 29 (6), 2008, 487-493.
- [3] Healy A., Moran K., Dickinson J., Hurley C., Smeaton A., O'Connor N., Kelly P., Haahr M., Chockalingam N., *Analysis of the 5 iron golf swing when hitting for maximum distance*, Journal of Sports Sciences, 29, 2011, 1079–1088.
- [4] Lukas T.D., *Computational modeling of the Golf Stroke*, PhD, Glasgow Theses Service, 1999.
- [5] Xu Z., *A Study of Impact between Golf Ball and Face of Golf Club Head*, BSc MEng Project Report, 2015, 1-21.
- [6] Maruoka K., Sakagami S., Yamada K., Nakagawa N., Sekiguti Y., *Dynamic Impact Characteristics of Golf Ball Materials*, Materials and Science in Sports, TMS, 2001, pp. 146-159.
- [7] Mase T., *Experimental Benchmarking Golf Ball Mechanical Properties*, X International Congress and Exposition on Experimental and Applied Mechanics, 2004.
- [8] Wu Z., Sogabe Y., Arimitsu Y., *Determination of Material Properties of Golf Ball and Optimization of Golf Clubhead*, SEM Annual Conference on Experimental and Applied Mechanics, Vol. 3, 2009, 1924-1931.
- [9] Alam F., Chowdhury H., Moria H., Bray R.L., Subic A., *A Comparative Study of Golf Ball Aerodynamics*, 17th Australian Fluid Mechanics Conference, Auckland, New Zealand, 5-9 December, 2010.
- [10] Kim J., Choi H., *Aerodynamics of a Golf Ball with Grooves*, Institution of Mechanical Engineers, Journal of Sports Engineering and Technology, 2014, Vol. 228, 4, 233-241.
- [11] Tai C.H., Leong J.C., Lin C.Y., *Effects of Golf Ball Dimple Configuration on Aerodynamics, Trajectory, and Acoustics*, Journal of Flow Visualization and Image Processing, 14 (2), 2007, 183-200.
- [12] Mehta R.D., Pallis J.M., *Sports ball aerodynamics: effects of velocity spin and surface roughness*, Materials and Science in Sports, pp 186-197, TMS, 2001, 185-197.
- [13] Penner A.R., *The physics of golf: The optimum loft of a driver*, American Journal of Physics, 69 (5), 2001, 563-568.
- [14] Barber R., *Golf Ball Flight Dynamics*, Cornell University, A&EP 434 Final Project, Professor Lovelace, 2007.
- [15] Baek S., Kim M., *Flight Trajectory of a Golf Ball for Realistic Games*, International Journal of Innovation, Management and Technology, Vol. 4, No. 3, 2013, 346-350.
- [16] Ivanov A.I., *Investigation of three-dimensional tennis ball flight*, Journal Mechanics of Machines, year XXII, book 2, 2014, 34-37. (in Bulgarian)
- [17] Nikolov S., Nedev V., *Bifurcation analysis and dynamic behaviour of an inverted pendulum with bounded control*, J. of Theoretical and Applied Mechanics, vol. 46, No 1, 2016, 17-32.
- [18] The Rules of Golf & Golf Equipment, Appendix III – The Ball, Available from: <http://www.randa.org/Rules-of-Golf/Appendices/Appendix-III-the-ball/>
- [19] Robinson G., Robinson I., *The motion of an arbitrarily rotating spherical projectile and its application to ball games*, Physica Scripta, Vol. 88, N 1, 2013, 018101, 17 p.